fire

MDPI

Article

Influence of Nano Composites on the Impact Resistance of Concrete at Elevated Temperatures

Balamurali Kanagaraj [1], Anand Nammalvar [1,*], A. Diana Andrushia [2], Beulah Gnana Ananthi Gurupatham [3] and Krishanu Roy [4,*]

1 Department of Civil Engineering, Karunya Institute of Technology and Sciences, Coimbatore 641114, India
2 Department of ECE, Karunya Institute of Technology and Sciences, Coimbatore 641114, India
3 Division of Structural Engineering, College of Engineering Guindy campus, Anna University, Chennai 600025, India
4 School of Engineering, The University of Waikato, Hamilton 3216, New Zealand
* Correspondence: nanand@karunya.edu (A.N.); krishanu.roy@waikato.ac.nz (K.R.)

Abstract: The addition of nanomaterials to concrete efficiently fills the pores of the concrete, thereby improving its hardening characteristics. However, no research is available in the literature that investigated the influence of nano-cement (NC), nano-silica-fume (NS), nano-fly-ash (NF), and nano-metakaolin (NM), which are used as partial replacements for cement, on the impact strength (IS) of concrete at elevated temperatures. This issue is addressed herein. Nanomaterials were used in this study to replace 10%, 20%, and 30% of the cement in four different grades of concrete, starting from M20 to M50, at different temperatures. This nano-blended matrix was exposed to various temperatures ranging from 250 °C to 1000 °C, with an increment of 250 °C. In total, the results of 384 new tests were reported. In addition, morphological changes undergone by the concrete specimens were observed through a scanning electron microscope (SEM). The study revealed that the type of binder, proportion of binder, heating intensity, duration, and cooling type directly influenced the impact strength of concrete when subjected to elevated temperature. In comparison to NC, NF, NS, and NM, the mix with NC possessed superior performance when it was heated at 1000 °C. Prior to being subjected to elevated temperatures, the MK blended concrete mix performed well; however, when subjected to elevated temperatures, the MK blended concrete also experienced severe damage.

Keywords: concrete; nanomaterials; elevated temperature; impact strength; microstructure

Citation: Kanagaraj, B.; Nammalvar, A.; Andrushia, A.D.; Gurupatham, B.G.A.; Roy, K. Influence of Nano Composites on the Impact Resistance of Concrete at Elevated Temperatures. *Fire* **2023**, *6*, 135. https://doi.org/10.3390/fire6040135

Academic Editor: Pinghua Zhu

Received: 1 March 2023
Revised: 19 March 2023
Accepted: 21 March 2023
Published: 27 March 2023

1. Introduction

With the increased number of catastrophic fires in structures, assessing fire-affected structures is a new area of research in the construction industry. Engineers and architects have difficulties in restoring the strength and appearance with the operation of a structure following fire exposure. Adequate design and material selection are the key factors to ensure the safety of the buildings under fire hazards. Fire protection codes and guidelines must be updated on a regular basis based on research findings [1]. Designers must fully understand the impact of fire on structural members to overcome failures when they are subjected to elevated temperatures for an extended period [1].

The capacity to withstand energy, often known as "toughness", is a basic design characteristic for structural members susceptible to impact stresses. Impact strength is the capacity of a material to bear an unexpected load and is defined in terms of its energy. Impact loads significantly deteriorate structural strength and result in a loss of functional stability and integrity. Some building components, such as airport runways, and beam-column junctions, when subjected to seismic loads, and abrupt explosions, must withstand the impact forces applied to those building components. Therefore, the impact resistance of concrete must be improved to withstand such frequently applied impact loads. High-performance concrete (HPC) is required for impact-resistant structures [2]. Its constituents and microstructure strongly influence the hardening characteristics of concrete. The calcium silicate hydrate (C-S-H) gel is vital for the strength development in concrete. Significant changes in strength and morphology can be seen when nanomaterials are employed as supplementary cementitious materials in concrete [3].

The use of nanomaterials can resist the alkali-silica reaction, rusting, and freeze-thaw characteristics of concrete, as well as minimize porosity and shrinkage occurrence [4]. Many researchers have examined the impact of various types of nanomaterials on the hardening characteristics of composites (paste, mortar, and concrete), namely nano-silica [5], nano-alumina [6], nano-Fe_2O_3 [7], and nano-titanium di-oxide [8]. Because of its strong cementitious nature and low cost, NS is the most extensively used nanomaterial. Furthermore, due to its strong pozzolanic activity, NS is combined with calcium hydroxide, which is formed during the hydration reaction process of cement, to form C-S-H gel [9].

However, there is no information in the literature on the optimal dose of such nanomaterials and the associated enhancement of the hardened properties of concrete, particularly its compressive strength (CS). Researchers [10] showed that the use of nano-silica and nano-titanium dioxide to replace cement by 3% could increase the CS by 15.5% and 8.6%, respectively. They also discovered that nano-silica improves the early strength while titanium dioxide has the opposite effect. The highest CS was achieved when nano-silica was employed at a dose of 0.5%, after which the gain in the CS was reduced [11]. Kanagaraj et al. [12] reported that incorporating NS into concrete enhanced its CS by up to 6% at all curing ages.

Concrete containing 30% fly ash (FA) and nano-silica showed significant enhancement in its CS at 28 days. Safiuddin et al. [13] investigated the effects of nano-silica and nano-alumina on the freeze and thaw resistance of concrete. The improvement in the 28-day CS was 30.13% when 5% nano-silica was employed, but the strength development was only 7.9% when 3% nano-alumina was used. Kanagaraj et al. [14] found that the inclusion of nano-silica increased the tensile strength (TS) and flexural strength (FS) of high-strength concrete (HSC) at 28 days by approximately 45% and 24%, respectively. The addition of fly ash to concrete as a partial replacement for cement increases matrix density, durability, and sustainability [15,16]. According to Naji Givi et al. [17], the optimal substitution of nano-silica was between 1% and 1.5%. According to researcher [12], the FS of high-performance concrete increased up to 1% with an increase in nano-silica dose, then decreased. Several researchers evaluated the mechanical characteristics of concrete with single nanomaterial while some used two materials. For example, using 6% NM and 0.02% carbon nanotubes together may raise the CS of concrete by 29% [18]. According to [19], adding hybrid nano-silica and nano-clay was found to improve the performance of regular cement pastes. Very few studies have explored the strength aspects of single nanomaterial-blended concretes at elevated temperatures and the strength parameters of nano-blended concrete at room temperature [20–22].

At 400 °C, 600 °C, and 800 °C, Bastami et al. [23] investigated the hardening characteristics of the nano-silica-blended HSC. The results show that nano-silica improves residual CS, reduces spalling, and reduces the mass loss in specimens by creating a denser internal structure. According to Heikal et al. [24], nano-alumina accelerates the hydration process of cement. For nano-alumina cement pastes without the superplasticizer, an increase in the nano-alumina content from 0 to 2% (with an increment of 1%) by mass was found to increase the CS by 10.89%, 31.03%, and 20.33%. However, at an elevated temperature of 450 °C, the rise in nano-alumina content from 0 to 2% increased the CS by 25.22%, 45.74%, and 28.49%, respectively. Horszczaruk et al. [25], on the other hand, concluded that nano-silica (up to 3%) improved the thermal resistance of mortars, particularly at temperatures up to 200 °C. However, at elevated temperatures ranging up to 400 °C, the impact is either negligible or not significant. Moreover, they have shown that nano-silica may react with lime to produce more C-S-H gel, thus improving the morphology of the matrix and reducing the risk of fracture propagation when exposed to elevated temperatures. When cement mortar was subjected to elevated temperatures of 200 °C, 400 °C, and 600 °C, Irshidat et al. [26]

demonstrated that including nano-clay significantly decreased the deterioration in the TS and FS of cement mortar. Additionally, scanning electron microscope (SEM) pictures showed that the density and length of hairline fractures that developed along the matrix due to the elevated temperature were less when nano-clay materials were added.

The aforementioned literature revealed that most studies focused on adding nanomaterials to regular cement paste or mortar and measuring its CS. Additionally, limited experiments are conducted with nanomaterials in concrete to examine their TS and FS. Therefore, the primary goal of this study is to determine the impact resistance of concrete blended with NC, NS, NF, and NM nanomaterials after being subjected to temperature exposure. The nanomaterials were used to replace 10%, 20%, and 30% of the cement in four different grades of concrete, ranging from M20 to M50, at various temperatures. This nano-blended matrix was subjected to temperatures ranging from 250 °C to 1000 °C, with increments of 250 °C. A total of 384 new tests were conducted, the results of which have been reported in this paper. Finally, the morphological changes of concrete specimens were determined using SEM.

2. Materials and Methods

2.1. Materials

Ordinary Portland cement (OPC) that complied with IS: 12269 [27] was used in this study. River sand (RS) was used as fine aggregate. RS has a specific gravity of 2.70 and complies with Zone-II of IS: 383:2016 [28]. The coarse aggregate (CA) had a specific gravity of 2.96. Class F-fly ash (FA) [29], silica fume (SF), and metakaolin (MK) were procured from the local market. Table 1 shows the physical and chemical properties of the cement, FA, SF, and MK.

Table 1. Chemical characteristics of cement, FA, SF, and MK.

Mineral Admixture	Cement	FA	SF	MK
Specific gravity	3.15	2.38	2.22	2.50
SiO_2 (%)	19.83	58.55	90.5	59.90
Fe_2O_3 (%)	3.53	3.44	0.8	1.28
Al_2O_3 (%)	13.5	28.20	0.7	32.29
CaO (%)	63.85	2.23	0.1	0.04
MgO (%)	0.52	0.32	0.30	0.17
Na_2O (%)	0.21	0.58	0.33	0.24
K_2O (%)	0.07	1.26	1.45	2.83
SO_3 (%)	2.43	0.07	-	-
Colour	gray	light gray	gray	white
Surface area (m^2/kg)	370	500–900	12,000	9000
Particle size (μm)	15–45	45–100	0.1	0.5

2.2. Methods

2.2.1. Mix Design

As mentioned above, OPC of grade 53 was used as the binder material of concrete in this study. Cement, FA, SF, and MK were ground in the ball-mill grinder to convert its macro-size particles to nano-size particles. After grinding, the nano-scaled materials were used in producing concrete of various proportions, including 10%, 20%, and 30%. Four concrete grades (M20, M30, M40, and M50) were used to study the influence of nanomaterials subjected to elevated temperatures. Table 2 shows the mix design adopted in this study.

Table 2. Mix design of concrete.

Mix ID	Cement	RS	CA	w/c Ratio	SP
	kg/m^3	kg/m^3	kg/m^3		kg/m^3
M20	320	850	1035	0.59	-
M30	380	800	1035	0.5	-
M40	410	800	1150	0.37	4.9
M50	460	770	1140	0.33	5.5

2.2.2. Details of the Furnace and Heating of Specimens

Four heating regimes were followed in the current study, namely, 250 °C, 500 °C, 750 °C, and 1000 °C. After being heated, the specimens were removed from the furnace in a hot state and were cooled by air or by spraying water. To heat the samples to the desired temperatures and duration, an electrical furnace with inner dimensions of 500 mm × 500 mm × 500 mm with a power capacity of 110 kW was used. The maximum heating capacity temperature of the furnace is 1250 °C. The furnace is equipped with a microcontroller that can be programmed to control the temperature. The furnace consists of coils on four sides that heat the specimens through radiation when the target temperature is set. The furnace has two displays: (a) set value display which records the specimen's temperature at different time intervals, and (b) program value display which shows the coils' temperature at a given time. After the temperature is set, the coil heats the specimens till the target time is reached, and then the furnace stops automatically.

In the case of air cooling, the specimens were kept in the furnace till it reached room temperature. For water cooling, the specimens were taken out from the furnace and water spraying was done under forced cooling.

Figure 1 depicts the furnace used and a photo of heated specimens cooled by means of air.

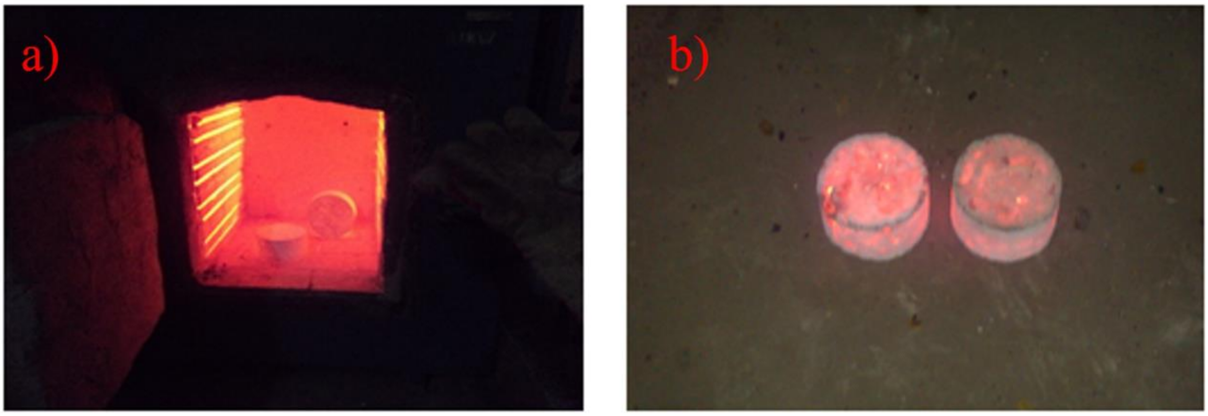

Figure 1. Photos of heated specimens. (**a**) Impact specimen under temperature exposure in furnace. (**b**) Air cooling of impact specimen.

2.2.3. Impact Strength (IS) Test of Heated Concrete Specimen

A number of researchers have assessed the concrete's IS. Due to its simple methodology, the impact (drop weight) test has been widely used in the industry and in academia. The IS test in this study was conducted in accordance with ACI 544 [30]. The test involved repeatedly striking a steel ball placed at the center of the cylindrical specimen with a 44.7 N hammer from a height of 457 mm. The specimens were 64 mm in height and had a diameter of 150 mm. The specimens were positioned between the three legs of the impact testing machine and set on the base plate, thereby ensuring the safety of the hammer when striking the steel ball. Two values that represent initial and final failure were recorded. The number of blows required to initiate the visible crack and the number required to break the specimen completely were noted. Based on the visual inspection, the first fracture was determined. The test specimen's surface was whitewashed to aid in spotting this break. According to the ACI guidelines [30], the ultimate failure happens when significant impact energy is used to expand the fractures so that the test specimen hits the steel lugs. The impact test configuration used in the experiments is illustrated in Figure 2.

Figure 2. Impact test set-up. (**a**) Initial crack; (**b**) Final failure.

In the current study, concrete was prepared by replacing cement partially with four different types of nanomaterials, NC, NF, NS, and NM. A total of 384 specimens were cast and tested. Table 3 shows the details of specimens used in the investigation.

Table 3. Details of cylindrical specimens used for finding impact strength.

Type of Nano Material	Concrete Grade	Percentage Replacement by Cement	Temperature	Cooling Type	No. of Specimens
Cement	M20	10%, 20%, and 30%	250 °C, 500 °C, 750 °C, and 1000 °C	Air	48
SF					
FA				Water	48
MK					
Cement	M30	10%, 20%, and 30%	250 °C, 500 °C, 750 °C, and 1000 °C	Air	48
SF					
FA				Water	48
MK					
Cement	M40	10%, 20%, and 30%	250 °C, 500 °C, 750 °C, and 1000 °C	Air	48
SF					
FA				Water	48
MK					
Cement	M50	10%, 20%, and 30%	250 °C, 500 °C, 750 °C, and 1000 °C	Air	48
SF					
FA				Water	48
MK					

Total number of cylindrical specimens cast and tested under impact loading.

2.2.4. Impact Strength of Concrete at Elevated Temperatures

The impact strength was measured in terms of energy; it is a material's capacity to sustain an abruptly applied load. The objective of this study is to understand the influence of nanomaterials in concrete and their effect at elevated temperatures. The most influencing factors affecting the IS of concrete are temperature, cooling regime, the type of nanomaterial, the content of powder in concrete, and the grade of concrete. The following equation was used to determine the impact energy;

$$E = m \times h \times n \text{ (Nm)} \quad (1)$$

where

m = weight of the hammer (N).
h = height of fall (m).
n = the number of blows required for ultimate failure.

3. Impact Test Results and Discussion

3.1. Effect of Temperature on the Impact Energy of Concrete with Different Nanomaterials

According to the findings from the experimental study, the energy loss was substantially above 250 °C and most pronounced between 750 °C and 1000 °C. From the results of the experiments, it was found that the heating rate and peak temperature are the two key parameters that significantly affect the impact energy of concrete. As the temperature rises, the impact energy decreases, as can be seen from the graphs (Figures 3–6). All grades of concrete that contained various types of nanomaterials exhibited the same behavior. Compared to other materials, concrete with NC and NF was found to have superior impact energy, while NM-blend concrete showed the lowest impact energy. In every instance, the impact energy of the concrete was found to be lower for specimens cooled by water than for specimens cooled by air. Figure 3 shows the impact energy of M20 grade concrete with varying proportions of nanomaterials (NC, NF, NM, and NS) starting from 10% to 30%.

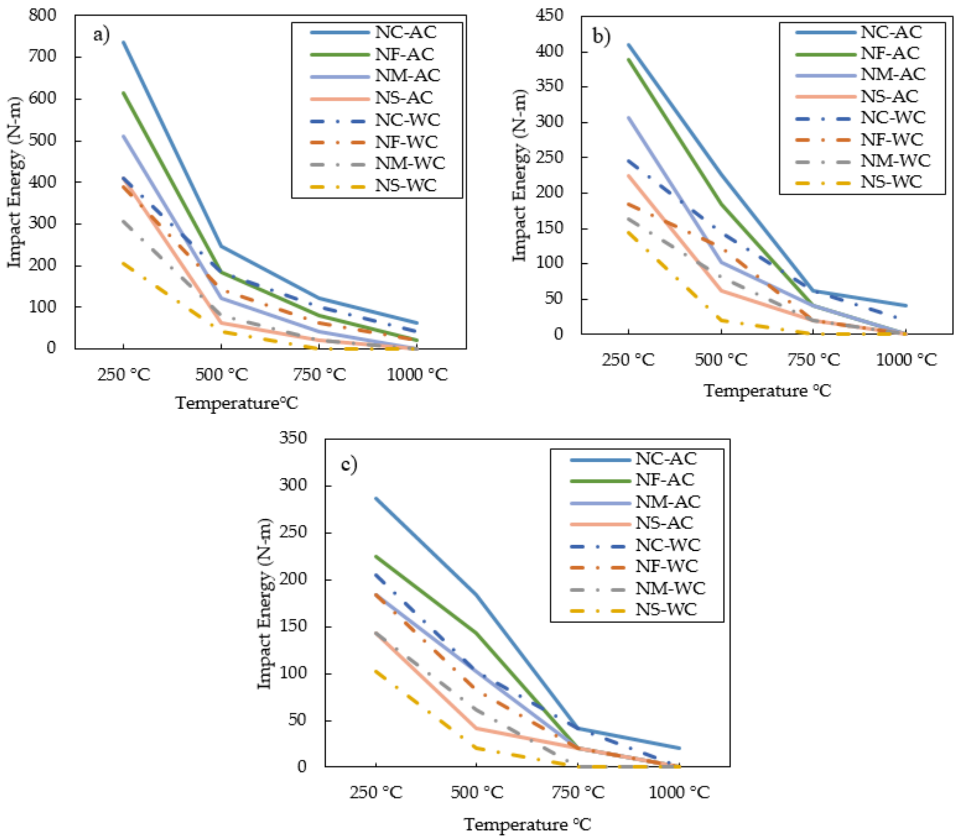

Figure 3. Impact energy versus temperature of M20 grade concrete with various percentages of nanomaterials: (**a**) 10%; (**b**) 20%; (**c**) 30%.

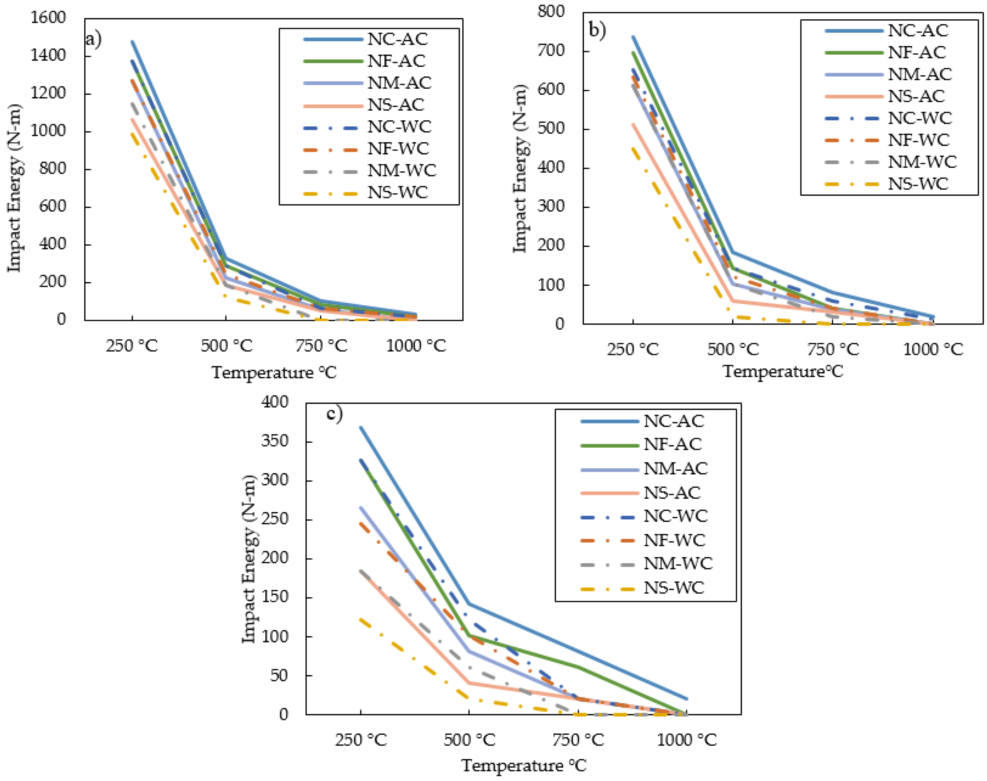

Figure 4. Impact energy versus temperature of M30 grade concrete with various percentages of nanomaterials: (**a**) 10%; (**b**) 20%; (**c**) 30%.

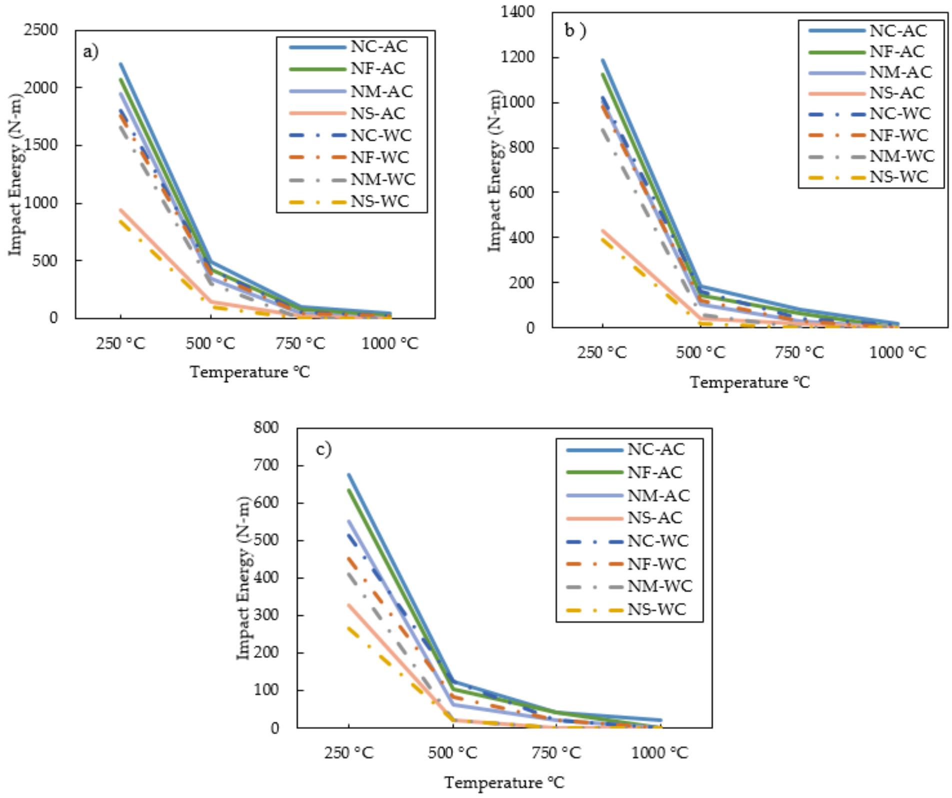

Figure 5. Impact energy versus temperature of M40 grade concrete with various percentages of nanomaterials: (**a**) 10%; (**b**) 20%; (**c**) 30%.

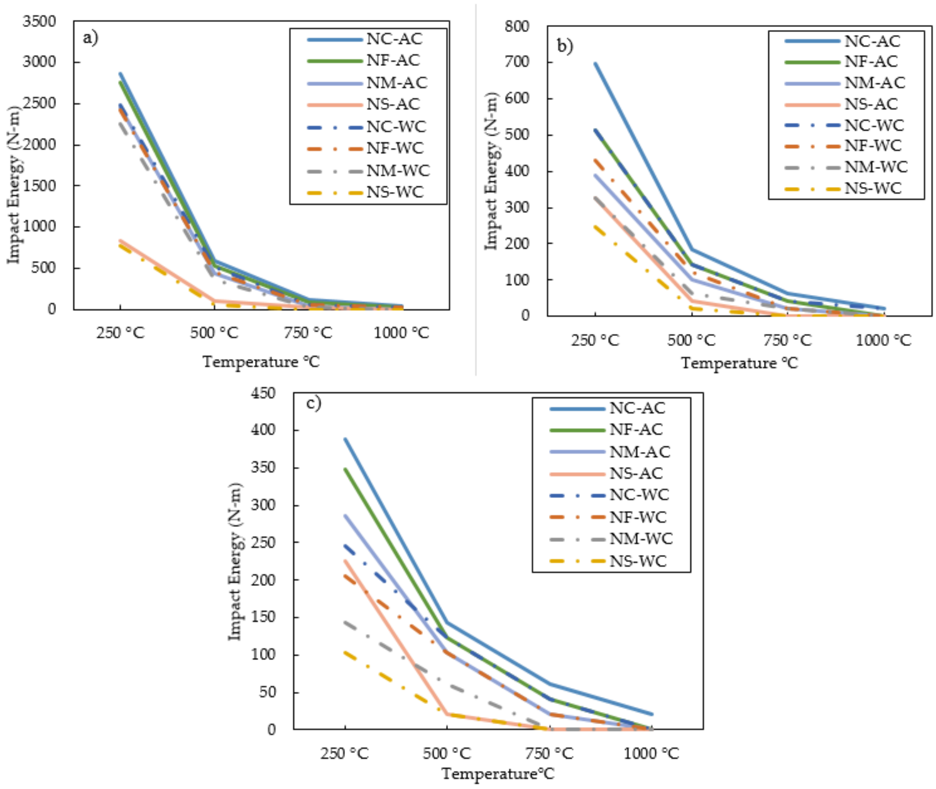

Figure 6. Impact energy versus temperature of M50 grade concrete with various percentages of nanomaterials: (**a**) 10%; (**b**) 20%; (**c**) 30%.

Similarly, Figures 4–6 show the impact energies of M30, M40, and M50 grades of concrete, respectively. Amongst all the concrete grades, the ones blended with NC performed better than the ones blended with NF, NM, and NS for the heating range from 250 °C to 1000 °C. Water-cooled (WC) specimens exhibited poorer performance than the air-cooled specimens; this might be attributed to the quenching effect [24]. Degradation of the C-S-H gel, thermal incompatibility between the filler and binder medium, and high pore pressure inside the cement paste all occurred when materials were exposed to elevated temperatures. The hardened cement pastes of higher-grade concrete generated higher pore pressure inside the HSC, preventing moisture vapor from evaporating at elevated temperatures. If the thermal stresses exceed the tensile strength of the concrete, micro-cracks will form, causing the concrete to spall, as was observed in the experiments.

Figures 7–10 illustrate the impact energy of various grades of concrete with respect to the percentage of nanomaterials at 250 °C, 500 °C, 750 °C, and 1000 °C, respectively. From the experimental results, it is found that concrete mix blended with 10% NC suffers an energy loss of 1.21%, 79.54%, 95.77%, and 98.59% when subjected to 250 °C, 500 °C, 750 °C, and 1000 °C, respectively, and cooled under the ambient temperature. In contrast, for water-cooled specimens, the energy loss was found to be 14.62%, 82.36%, 97.88%, and 99.29%, respectively, as illustrated in Table 4. This shows that the water-cooled specimens had more energy loss than the air-cooled specimens. This might be attributed to a sudden drop in the surface temperature that causes higher thermal incompatibility inside the concrete [31]. Air-cooled concrete mix with 30% NC had an energy loss percentage between 5.17% and 95.01% (for the temperature range of 250 °C to 1000 °C). However, in case of the water-cooled specimens, the energy loss was found to be 10.11% to 100% (for the temperature ranging from 250 °C to 1000 °C).

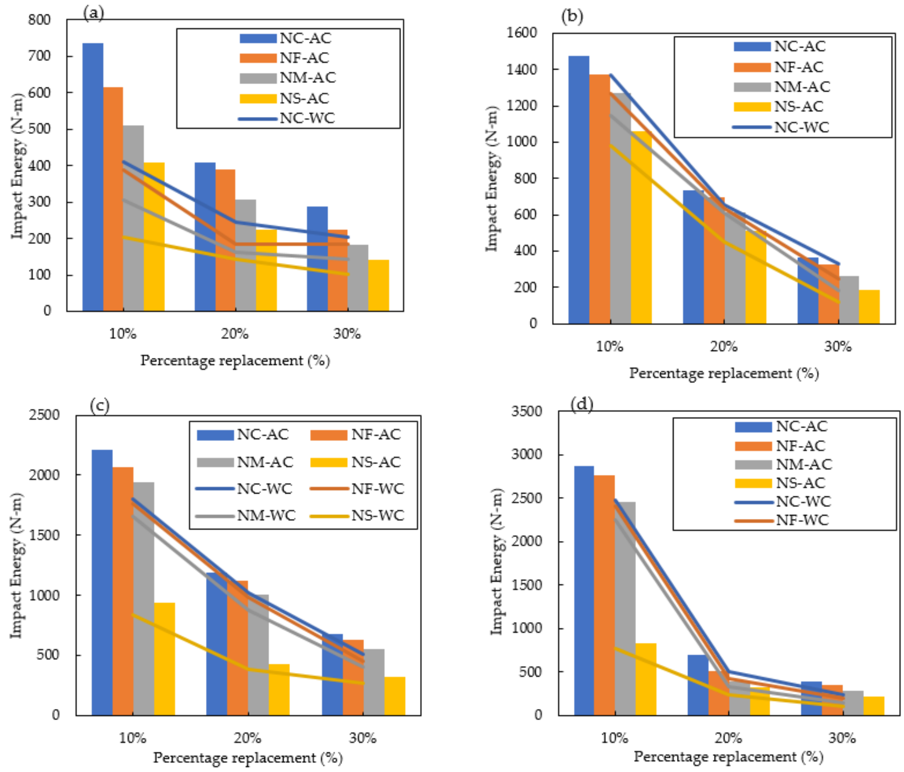

Figure 7. Impact energy versus percentages of nanomaterials in various grades at 250 °C: (**a**) M20; (**b**) M30; (**c**) M40; (**d**) M50.

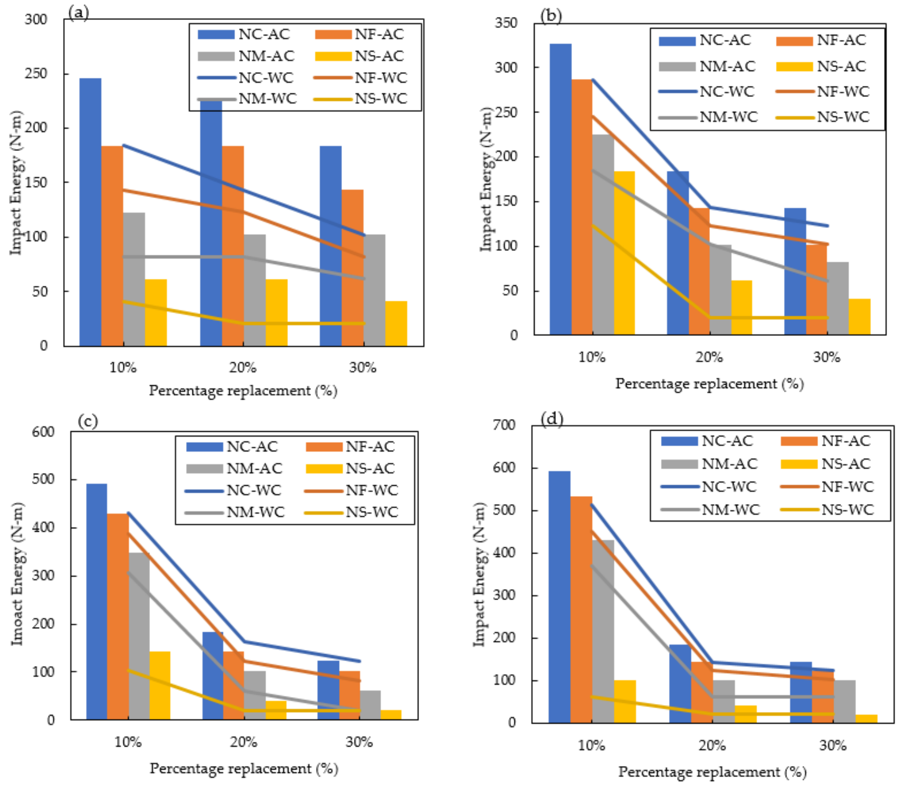

Figure 8. Impact energy versus percentages of nanomaterials in various grades at 500 °C: (**a**) M20; (**b**) M30; (**c**) M40; (**d**) M50.

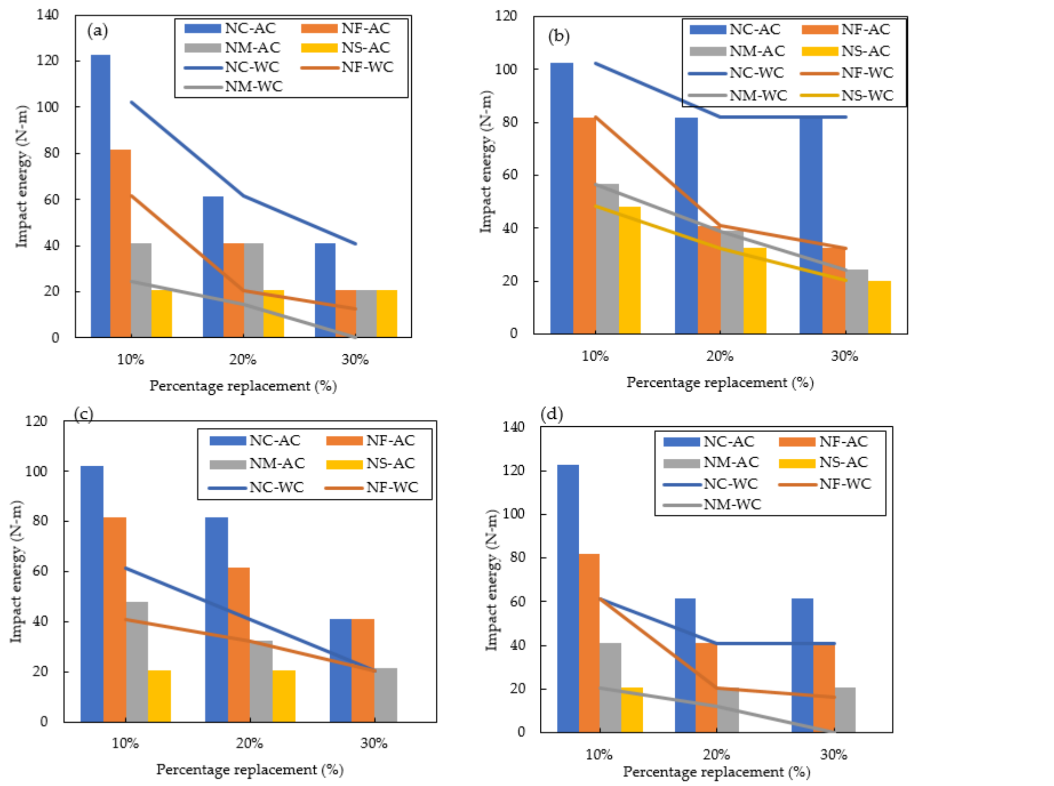

Figure 9. Impact energy versus percentages of nanomaterials in various grades at 750 °C: (**a**) M20; (**b**) M30; (**c**) M40; (**d**) M50.

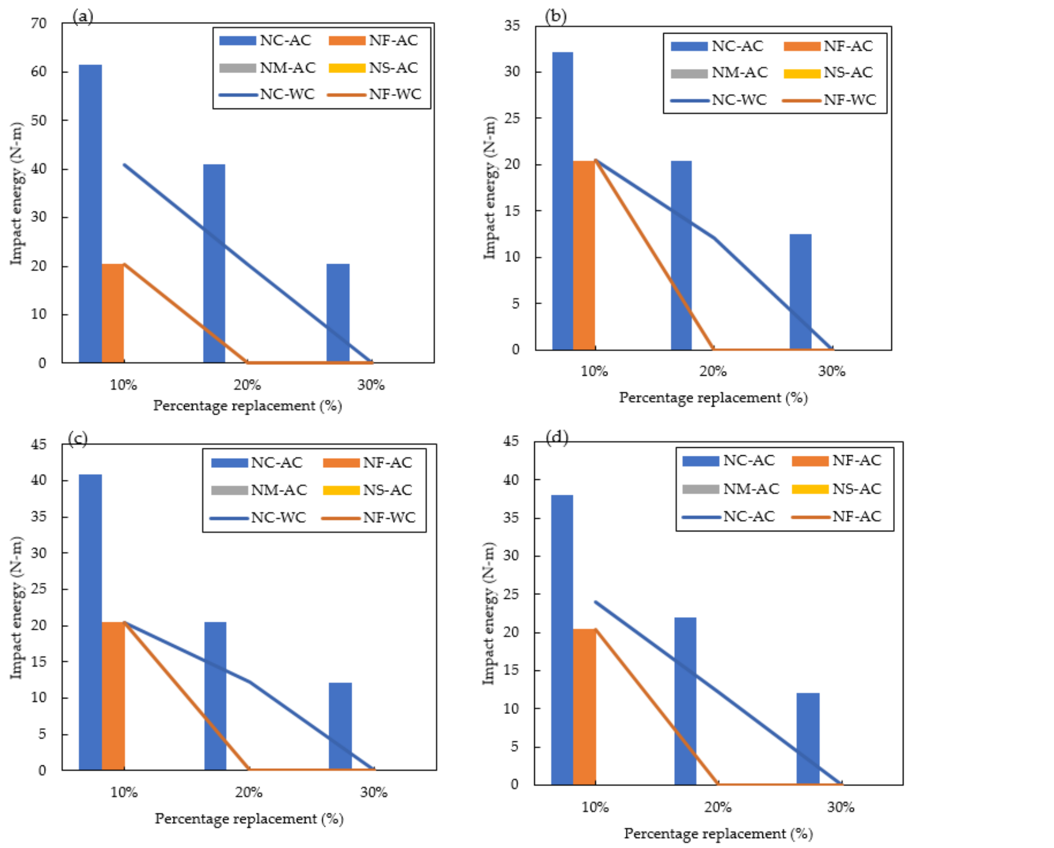

Figure 10. Impact energy versus percentages of nanomaterials in various grades at 1000 °C: (**a**) M20; (**b**) M30; (**c**) M40; (**d**) M50.

Table 4. The impact energy of specimens cast with NC.

Temperature (°C)	Impact Energy (IE) of M20 Concrete Specimens											
	10% Replacement of NC				20% Replacement of NC				30% Replacement of NC			
	AC	Loss of IE (%)	WC	Loss of IE (%)	AC	Loss of IE (%)	WC	Loss of IE (%)	AC	Loss of IE (%)	WC	Loss of IE (%)
IE of reference specimen (Ambient temperature)	2900				705				410			
250	2864	1.21	2476	15	695	1	511	27	388	5	245	40
500	593	80	511	82	184	74	143	80	143	65	122	70
750	122	96	61	98	61	91	40	94	61	85	40	90
1000	40	99	20	99	20	97	20	97	20	95	0	100

In the case of the air-cooled concrete mix blended with 10% NF, the energy loss was found to be 2.07% to 99.27% (for the temperature ranging from 250 °C to 1000 °C). For the water-cooled specimens, the energy loss was found to be between 14.40% and 99.27% (for the temperature ranging from 250 °C to 1000 °C). For an air-cooled concrete mix blended with 30% NF, the energy loss percentage was found to range between 4.69% and 100%, however, for water-cooled specimens, the energy loss percentage was found to range from 43.93% to 100% (as given in Table 5). In the case of a concrete mix blended with 10% NS, the energy loss was found to range from 2.75% to 100% for air-cooled specimens. In the case of water-cooling, the loss was found to vary between 10.85% and 100% (as given in Table 6). For the mix with 30% NS, the energy loss was found to be between 5.76% to 100% for the air-cooled specimens and 52.88% to 100% for the water-cooled specimens.

Table 5. The impact energy of specimens cast with NF.

Temperature (°C)	Impact Energy Of M30 Concrete Specimens											
	10% Replacement of NF				20% Replacement of NF				30% Replacement of NF			
	AC	Loss of IE (%)	WC	Loss of IE (%)	AC	Loss of IE (%)	WC	Loss of IE (%)	AC	Loss of IE (%)	WC	Loss of IE (%)
IE of reference specimen (Ambient temperature)	2821				538				365			
250	2762	2	2414	14	511	4	429	20	347	4	204	44
500	532	81	450	84	143	73	122	77	122	6	102	72
750	81	97	61	97	40	92	20	96	40	89	20	94
1000	20	99	20	99	0	100	0	100	0	100	0	100

The loss in the impact energy the concrete mix blended with 10% NM was observed to be in the range 5.20% and 100% for air-cooled specimens and from 12.13% to 100% for the water-cooled specimens. The impact energy loss of the concrete mix blended with 30% NM varied from 6.21% to 100% for the air-cooled specimens and from 57.37% to 100% for the water-cooled specimens as given in Table 7.

Table 6. The impact energy of specimens cast with NS.

Temperature (°C)	Impact Energy of M40 Concrete Specimens											
	10% Replacement of NS				20% Replacement of NS				30% Replacement of NS			
	AC	Loss of IE (%)	WC	Loss of IE (%)	AC	Loss of IE (%)	WC	Loss of IE (%)	AC	Loss of IE (%)	WC	Loss of IE (%)
IE of reference specimen (Ambient temperature)	2525				403				304			
250	2455	3	2251	11	388	3	327	18	286	5	143	53
500	429	83	368	85	102	74	61	84	102	66	61	80
750	40	98	20	99	20	94	20	94	20	93	0	100
1000	0	100	0	100	0	100	0	100	0	100	0	100

Table 7. Impact energy of specimens cast with NM.

Temperature (°C)	Impact Energy of M50 Concrete Specimens											
	10% Replacement of NM				20% Replacement of NM				30% Replacement of NM			
	AC	Loss of IE (%)	WC	Loss of IE (%)	AC	Loss of IE (%)	WC	Loss of IE (%)	AC	Loss of IE (%)	WC	Loss of IE (%)
IE of reference specimen (Ambient temperature)	885				348				240			
250	839	5	777	12	327	6	245	29	225	6	102	57
500	102	88	61	93	40	88	20	94	20	91	20	91
750	20	98	0	100	0	100	0	100	0	100	0	100
1000	0	100	0	100	0	100	0	100	0	100	0	100

According to Nadeem's experiments [32], concrete containing FA performed better than concrete with MK at and above 400 °C. The IS of concrete with MK was also discovered to be nearly zero in the current investigation. This is a caution that MK blends should be used carefully, particularly in construction that may be exposed to temperatures of 400 °C or higher [33]. Morsy [34] stated that the CS of specimens reduced significantly at elevated temperatures above 250 °C. According to the findings of Kodur and Agarwal [35], impact energy decreased for the specimens exposed to 500 °C compared to the reference specimen.

At a temperature of 400 °C to 450 °C, C-S-H deteriorates to CaO with a volume reduction of 44% [36]. The performance of OPC decreases at elevated temperatures up to 400 °C due to the chemical and physical changes in the hydrated phases of the binder. Dehydration and loss of chemically bonded water are caused by heat exposure, mostly due to the dihydroxylation of CH, which reduces the chemical bonding and strength [35–39]. Gel-like hydration products disintegrated at 400 °C. $CaCO_3$ dissociates into CaO and CO_2 at 600 °C. Between 600 and 800 °C, re-crystallization of non-binding phases from hydrated cement during re-heating was observed [39]. The C-S-H gels were fully destroyed at 900 °C after continuing to dehydrate and decompose [40].

The C-S-H gel was formed during the hydration of cementitious ingredients and water, which helped in achieving good hardening properties of the concrete. Free water in the concrete mix evaporates at elevated temperatures ranging from 150 to 300 °C. Hydrates get dissolved, and chemically bonded water evaporates as the temperature increases. The breakdown of CaOH begins around 350 °C, while the partial volatilization of C-S-H gel starts at about 500 °C, according to experimental data from [41,42]. As a result, the mechanical properties of the hydrates are impaired; also, the pore size and porosity of the hydrated matrix increase [43]. Additionally, the aggregates expand beyond 600 °C due to low specific heat and a rapid thermal expansion rate, increasing the volume of concrete. With all these modifications, the mechanical properties of heated concrete become temperature dependent. Due to the dissolution of C-S-H gel, all forms of concrete showed serious degradation at 800 °C [44]. The current experimental tests confirmed these findings.

3.2. Effect of the Percentages of Replacement of Nanomaterials/Powder Content on the IS of Concrete

It is well known that the density of concrete will increase with the concrete grade due to its increased powder content [45]. The current experimental study demonstrates the impact of powder content on the IS of heated concrete. The data shows that concrete's impact energy decreases as powder concentration increases. This rate of decline is found to be greater with rising temperatures and better-quality concrete. The type of additive used in the concrete specimens also significantly influences the impact energy of concrete when subjected to elevated temperatures.

The spalling of denser concrete at a moisture level of less than 3% by weight was not observed [46]. NS-containing concrete was more severely affected than any other nanomaterial. Adding various nanomaterials to cement paste improves the concrete's compressive strength, lowers permeability, and creates a denser microstructure. However, in heated specimens, additional fine powdered particles enter the pores of the concrete, increasing the pore pressure during heating (beyond 600 °C), which causes the concrete to spall [47].

From the experimental investigation, it was found that adding SF significantly densifies the concrete, which can lead to explosive spalling as a result of steam building up inside the pores, as shown in Figure 11. Furthermore, such concrete may be inferior to standard concrete when subjected to elevated temperatures, as the evaporation of physically absorbed water begins at 80 °C and causes thermal fractures. In addition, the results revealed that the ingredients of concrete, such as cement and admixtures, significantly impacted the fire resistance of concrete.

Figure 11. Failure pattern of specimens after impact testing at elevated temperatures. (**a**) Reference specimen at ambient temparature after testing. (**b**) Impact specimens exposed to 750 °C. (**c**) Impact specimens exposed to 1000 °C.

The impact energy reduction in concrete with SF is noticeably higher than those in concrete with NC, NF, and NM. This is linked to the presence and quantity of SF in concrete, which formed an extremely thick transition zone between aggregates and paste due to its ultra-fine filler particles and pozzolanic reactions. As a result, higher stress concentrations are created in the transition zone during aggregate expansion and paste contraction. Further, the bonding between filler and binder medium containing SF is more sensitive in OPC concrete. Thus, SF concrete has greater strength losses.

When high-strength concrete is made with the silica-fume-dense matrix, it is likely to spall when heated. The high density of the mix prevents the steam produced during heating from escaping, leading to explosive spalling.

Based on the tests conducted in this study, it can be concluded that the presence of SF, when subjected to elevated temperatures, has a greater detrimental influence on the IS of concrete. Concrete with NM has a fairly high impact energy compared to concrete with NS and a lower impact energy than concrete with NC and NF. Unlike other concrete mixes, MK concrete incurred more strength loss and had lower residual strengths. The major reasons for the poor performance of concrete with MK at elevated temperatures are its dense microstructure and low porosity. Compared to its mechanical strength, this concrete demonstrated a greater loss of impermeability.

Through two processes, NM increases the CS and FS of cement mortar [48]. The first process involves filling of the interstitial spaces inside the hardened cement with NM particles, thus increasing its density and strength. The second process creates more C-S-H gel through a pozzolanic interaction between NM and the free CH released after concrete's hydration of OPC. The dehydration process of the produced hydrate relates to the release of free water when a denser structure is subjected to high temperatures. The residual fraction of water causes the creation and growth of microcracks. High thermal stresses caused by induced temperature gradients up to 800 °C led to enhanced microcracking [49]. The calcium oxide changes back into calcium hydroxide if wetted after cooling or the atmosphere is humid. These volume variations can disintegrate the concrete. The increase in peak strain is due to fissures caused by the thermal incompatibility of the aggregates and the cement paste during heating and cooling. Due to the formation of microcracks and brittle microstructure, the concrete mixes were more damaging when the specimens were subjected to tensile stress. Concrete that was cooled in water as opposed to air showed a significant drop in strength, likely owing to micro-cracks development by applying thermal shock to the heated specimens.

According to the current investigation, elevated temperatures may have caused micro- and macro-cracks to form in mortars made of various nanomaterials. The particle size of cement is below 75 µm, and for fly ash, it is less than 100 µm. Whereas in the case of silica fume and metakaolin, the particle sizes are from 0.1 to 0.3 µm and less than 5 µm, respectively. FA, SF, and MK have respective surface areas of 370 m^2/kg, 500 m^2/kg, 12,000 m^2/kg, and 9000 m^2/kg. Despite having smaller particles than cement, FA, MK, and SF make the concrete mix more solid, compact, and impenetrable due to their high powder concentration. When the temperature is too high, water vapor cannot escape from the concrete containing SF, which raises the pore pressure and causes explosive spalling.

4. Microstructure Investigation

The scanning electron microscope (SEM) analysis was performed to study the internal morphology of the concrete mix blended with and without nanomaterials. Moreover, SEM analysis was also used to examine the presence of hydrated C-S-H gel phases. This is to examine the microstructure of the concrete mix blended with nanomaterials. The morphological changes of the concrete mix that were exposed to elevated temperatures were analyzed.

SEM

The SEM morphology of concrete before exposing it to an elevated temperature is shown in Figure 12, where it can be seen that the dense internal structure of the concrete mix is blended with nanomaterials, which might be attributed to the pore-filling ability of nano-scaled particles. Figure 12a depicts the concrete mix blended without nanomaterials, while Figure 12b–e represents the concrete mix blended with 30% NC, NF, NS, and NM materials, respectively, before they were exposed to elevated temperatures. Figure 13 depicts the concrete specimens heated at 1000 °C and then cooled by air. The heated concrete specimens without nanomaterials exhibit considerable differences in microstructure, as shown in the aforementioned images. The occurrence of micro-cracks mixed with voids owing to increased porosity and the deformed CH and C-S-H gel is caused by an increase in temperature up to 1000 °C [47]. In addition, due to the rise in porosity, micro-cracks, and broken C-S-H phase boundaries, the micrograph displays significant changes in the microstructure.

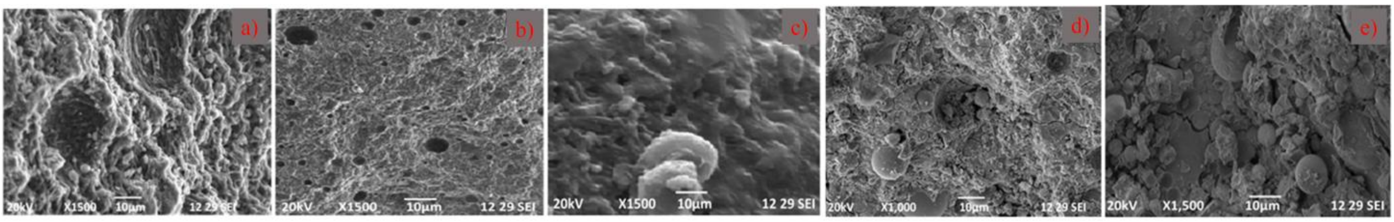

Figure 12. SEM images before exposure; (**a**) concrete without nanomaterials; (**b**) concrete with NC; (**c**) concrete with NF; (**d**) concrete with NS; (**e**) concrete with NM.

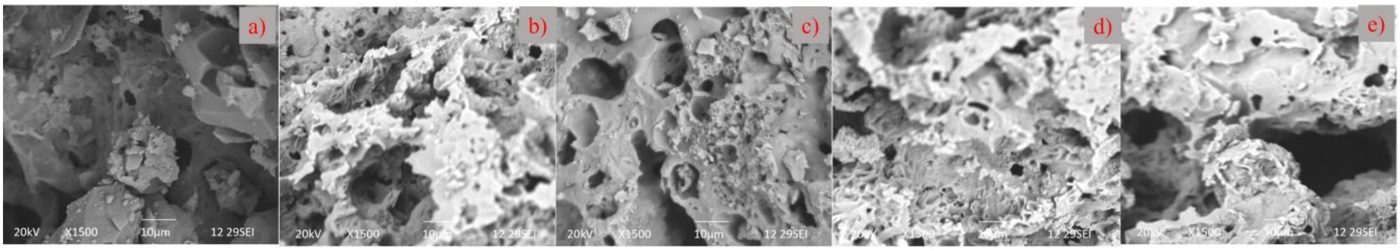

Figure 13. SEM images of concrete specimens exposed to elevated temperature 1000 °C; (**a**) concrete without nanomaterials; (**b**) concrete with NC; (**c**) concrete with NF; (**d**) concrete with NS; (**e**) concrete with NM.

Comparing Figures 12 and 13, it can be seen that the concrete specimens exposed to elevated temperatures show more pores. Due to its thermal incompatibility, the water molecules inside the concrete mix may experience internal pressure. This internal pressure tends to separate the binder and filler materials, causing larger cracks and leading to strength reduction. Significant amounts of free calcium hydroxide are present in hydrated Portland cement, and at around 400–450 °C, water loss causes calcium hydroxide to break down into calcium oxide. This calcium oxide increases its density as it reacts with a moist environment to change back into calcium hydroxide. Any possible volume changes can disintegrate the concrete [48]. A higher reduction in IS was seen in the concrete mix cooled in water than in the concrete mix cooled in air. This is due to micro-cracks created by thermal shocks while cooling the heated specimens [49].

5. Conclusions

The current investigation aims to study the effects of replacement of cement with 10%, 20%, and 30% nanomaterials (NC, NF, NS, and NM) at various temperatures. An electrical furnace was used to heat specimens of different grades of concrete (M20, M30, M40, and M50), which were subjected to temperatures of 250 °C, 500 °C, 750 °C, and 1000 °C. The following conclusions are drawn based on the outcome of this work:

- The strength of unheated concrete specimens containing nanomaterials increases as the proportion of nanomaterials increases.
- An increase in temperature from 250 °C to 1000 °C results in a decrease of the impact strength.
- The loss in impact strength of the concrete mix was influenced by binder type, proportion, heating intensity, duration, and cooling type.
- After exposure to elevated temperature, the performance of MK blended concrete was worse than that of the other concretes made with NC, NF, and NS. Concrete with MK was more vulnerable to elevated temperatures.
- The optimal dose of NM in the case of temperature exposure was found to be 10%. An increase in the proportion beyond 10% was good up to a temperature of 500 °C.

- In comparison with NC, NF, NS, and NM, the mix with NC exhibited superior performance when subjected to 1000 °C. Prior to exposure to elevated temperatures, the MK blended concrete mix performed well; however, when subjected to elevated temperatures, the MK blended mix was prone to severe damage.

Author Contributions: B.K., A.N., A.D.A.: Investigation, Methodology, Writing-original draft, review & editing. A.N., B.G.A.G., K.R.: Resources, Supervision. B.K., A.N., A.D.A.: Conceptualization. A.N., B.G.A.G., K.R.: Validation, suggested and chose the journal for submission. A.N., B.G.A.G., K.R.: Collaborated, Co-ordinated the research, Reviewed for submission. All authors have read and agreed to the published version of the manuscript.

Funding: This research received no external funding.

Institutional Review Board Statement: Not applicable.

Informed Consent Statement: Not applicable.

Data Availability Statement: The data presented in this study are available on request from the corresponding author.

Conflicts of Interest: The authors declare no conflict of interest.

References

1. Farmani, M.A.; Heidarpour, A. Development of Design Equations for Ultra-High Strength Steel CHS Columns under Transient Fire Conditions Considering Thermal Creep and Axial Restraint Effects. *Fire Saf. J.* **2023**, *136*, 103756. [CrossRef]
2. Bensalem, H.; Djaknoun, S.; Ouedraogo, E.; Amrouche, R. Analysis of Thermal-Induced Spalling Tests on High to Ultra-High Performance Concrete Subjected to Standard Fire. *Case Stud. Constr. Mater.* **2021**, *15*, e00704. [CrossRef]
3. Melo, J.; Triantafyllidis, Z.; Rush, D.; Bisby, L.; Rossetto, T.; Arêde, A.; Varum, H.; Ioannou, I. Cyclic Behaviour of As-Built and Strengthened Existing Reinforced Concrete Columns Previously Damaged by Fire. *Eng. Struct.* **2022**, *266*, 114584. [CrossRef]
4. Praveen Kumar, V.V.; Dey, S. Study on Strength and Durability Characteristics of Nano-Silica Based Blended Concrete. *Hybrid Adv.* **2023**, *2*, 100011. [CrossRef]
5. Nigam, M.; Verma, M. Effect of Nano-Silica on the Fresh and Mechanical Properties of Conventional Concrete. *Forces Mech.* **2023**, *10*, 100165. [CrossRef]
6. Younus, S.J.; Mosaberpanah, M.A. The Performance of Alkali-Activated Self-Compacting Concrete with and without Nano-Alumina. *Sustainability* **2023**, *15*, 2811. [CrossRef]
7. Abdalla, J.A.; Thomas, B.S.; Hawileh, R.A.; Yang, J.; Jindal, B.B.; Ariyachandra, E. Influence of Nano-TiO_2, Nano-Fe_2O_3, Nanoclay and Nano-$CaCO_3$ on the Properties of Cement/Geopolymer Concrete. *Clean. Mater.* **2022**, *4*, 100061. [CrossRef]
8. Choi, H.J.; Yoo, D.Y.; Park, G.J.; Park, J.J. Photocatalytic High-Performance Fiber-Reinforced Cement Composites with White Portland Cement, Titanium Dioxide, and Surface Treated Polyethylene Fibers. *J. Mater. Res. Technol.* **2021**, *15*, 785–800. [CrossRef]
9. Syamsunur, D.; Wei, L.; Ahmed Memon, Z.; Surol, S.; Md Yusoff, N.I. Concrete Performance Attenuation of Mix Nano-SiO_2 and Nano-$CaCO_3$ under High Temperature: A Comprehensive Review. *Materials* **2022**, *15*, 7073. [CrossRef]
10. Sikora, P.; Horszczaruk, E.; Rucinska, T. The Effect of Nanosilica and Titanium Dioxide on the Mechanical and Self-Cleaning Properties of Waste-Glass Cement Mortar. *Procedia Eng.* **2015**, *108*, 146–153. [CrossRef]
11. Guler, S.; Türkmenoğlu, Z.F.; Ashour, A. Performance of Single and Hybrid Nanoparticles Added Concrete at Ambient and Elevated Temperatures. *Constr. Build. Mater.* **2020**, *250*, 27–30. [CrossRef]
12. Kanagaraj, B.; Lubloy, E.; Anand, N.; Hlavicka, V.; Kiran, T. Investigation of Physical, Chemical, Mechanical, and Microstructural Properties of Cement-Less Concrete—State-of-the-Art Review. *Constr. Build. Mater.* **2023**, *365*, 130020. [CrossRef]
13. Safiuddin, M.; Gonzalez, M.; Cao, J.; Tighe, S.L. State-of-the-Art Report on Use of Nano-Materials in Concrete. *Int. J. Pavement Eng.* **2014**, *15*, 940–949. [CrossRef]
14. Kanagaraj, B.; Anand, N.; Andrushia, D.; Mathews, M.E.; Alengaram, J.; Arulraj, P.; Kiran, T. Mechanical Properties and Microstructure Characteristics of Self-Compacting Concrete with Different Admixtures Exposed to Elevated Temperatures. *Jordan J. Civ. Eng.* **2023**, *17*, 1–9. [CrossRef]
15. Rajamony Laila, L.; Gurupatham, B.G.A.; Roy, K.; Lim, J.B.P. Influence of Super Absorbent Polymer on Mechanical, Rheological, Durability, and Microstructural Properties of Self-Compacting Concrete Using Non-Biodegradable Granite Pulver. *Struct. Concr.* **2021**, *22*, E1093–E1116. [CrossRef]
16. Rajamony Laila, L.; Gurupatham, B.G.A.; Roy, K.; Lim, J.B.P. Effect of Super Absorbent Polymer on Microstructural and Mechanical Properties of Concrete Blends Using Granite Pulver. *Struct. Concr.* **2021**, *22*, E898–E915. [CrossRef]
17. Naji Givi, A.; Abdul Rashid, S.; Aziz, F.N.A.; Salleh, M.A.M. Experimental Investigation of the Size Effects of SiO_2 Nano-Particles on the Mechanical Properties of Binary Blended Concrete. *Compos. Part B Eng.* **2010**, *41*, 673–677. [CrossRef]
18. Pacheco-Torgal, F.; Miraldo, S.; Ding, Y.; Labrincha, J.A. Targeting HPC with the Help of Nanoparticles: An Overview. *Constr. Build. Mater.* **2013**, *38*, 365–370. [CrossRef]

19. Zhao, Z.; Qi, T.; Zhou, W.; Hui, D.; Xiao, C.; Qi, J.; Zheng, Z.; Zhao, Z. A Review on the Properties, Reinforcing Effects, and Commercialization of Nanomaterials for Cement-Based Materials. *Nanotechnol. Rev.* **2020**, *9*, 349–368. [CrossRef]
20. Nalon, G.H.; Ribeiro, J.C.L.; de Araújo, E.N.D.; Pedroti, L.G.; de Carvalho, J.M.F.; Santos, R.F.; de Oliveira, D.S. Residual Mechanical Properties of Mortars Containing Carbon Nanomaterials Exposed to High Temperatures. *Constr. Build. Mater.* **2021**, *275*, 122123. [CrossRef]
21. Polat, R.; Qarluq, A.W.; Karagöl, F. Influence of Singular and Binary Nanomaterials on the Physical, Mechanical and Durability Properties of Mortars Subjected to Elevated Temperatures and Freeze–Thaw Cycles. *Constr. Build. Mater.* **2021**, *295*, 123608. [CrossRef]
22. Iqbal, H.W.; Khushnood, R.A.; Latif Baloch, W.; Nawaz, A.; Tufail, R.F. Influence of Graphite Nano/Micro Platelets on the Residual Performance of High Strength Concrete Exposed to Elevated Temperature. *Constr. Build. Mater.* **2020**, *253*, 119029. [CrossRef]
23. Bastami, M.; Baghbadrani, M.; Aslani, F. Performance of Nano-Silica Modified High Strength Concrete at Elevated Temperatures. *Constr. Build. Mater.* **2014**, *68*, 402–408. [CrossRef]
24. Heikal, M.; Morsy, M.S.; Aiad, I. Effect of Treatment Temperature on the Early Hydration Characteristics of Superplasticized Silica Fume Blended Cement Pastes. *Cem. Concr. Res.* **2005**, *35*, 680–687. [CrossRef]
25. Horszczaruk, E. Properties of Cement-Based Composites Modified with Magnetite Nanoparticles: A Review. *Materials* **2019**, *12*, 326. [CrossRef] [PubMed]
26. Irshidat, M.R.; Al-Saleh, M.H. Thermal Performance and Fire Resistance of Nanoclay Modified Cementitious Materials. *Constr. Build. Mater.* **2018**, *159*, 213–219. [CrossRef]
27. *IS-12269*; 2004 Specification for 53 Grade Ordinary Portland Cement. Bureau of Indian Standards: New Delhi, India, 2004.
28. *IS 383*; Coarse and Fine Aggregate for Concrete-Specification. Bureau of Indian Standards: New Delhi, India, 2016.
29. Kanagaraj, B.; Anand, N.; Johnson Alengaram, U.; Samuvel Raj, R.; Kiran, T. Exemplification of Sustainable Sodium Silicate Waste Sediments as Coarse Aggregates in the Performance Evaluation of Geopolymer Concrete. *Constr. Build. Mater.* **2022**, *330*, 127135. [CrossRef]
30. ACI 544.2R-89 Measurement of Properties of Fiber Reinforced Concrete. *Am. Concr. Inst.* **1999**, *89*, 433–439.
31. Kanagaraj, B.; Anand, N.; Andrushia, A.D.; Lubloy, E. Investigation on Engineering Properties and Micro-Structure Characteristics of Low Strength and High Strength Geopolymer Composites Subjected to Standard Temperature Exposure. *Case Stud. Constr. Mater.* **2022**, *17*, e01608. [CrossRef]
32. Nadeem, A.; Memon, S.A.; Lo, T.Y. The Performance of Fly Ash and Metakaolin Concrete at Elevated Temperatures. *Constr. Build. Mater.* **2014**, *62*, 67–76. [CrossRef]
33. Nadeem, A.; Memon, S.A.; Lo, T.Y. Evaluation of Fly Ash and Metakaolin Concrete at Elevated Temperatures through Stiffness Damage Test. *Constr. Build. Mater.* **2013**, *38*, 1058–1065. [CrossRef]
34. Morsy, M.S.; Al-Salloum, Y.A.; Abbas, H.; Alsayed, S.H. Behavior of Blended Cement Mortars Containing Nano-Metakaolin at Elevated Temperatures. *Constr. Build. Mater.* **2012**, *35*, 900–905. [CrossRef]
35. Kodur, V.K.R.; Agrawal, A. Effect of Temperature Induced Bond Degradation on Fire Response of Reinforced Concrete Beams. *Eng. Struct.* **2017**, *142*, 98–109. [CrossRef]
36. Phan, L.T.; Lawson, J.R.; Davis, F.L. Effects of Elevated Temperature Exposure on Heating Characteristics, Spalling, and Residual Properties of High Performance Concrete. *Mater. Struct. Constr.* **2001**, *34*, 83–91. [CrossRef]
37. Vodák, F.; Trtík, K.; Kapičková, O.; Hošková, Š.; Demo, P. The Effect of Temperature on Strength-Porosity Relationship for Concrete. *Constr. Build. Mater.* **2004**, *18*, 529–534. [CrossRef]
38. Schneider, U.; Diederichs, U.; Ehm, C. Effect of Temperature on Steel and Concrete for PCRV's. *Nucl. Eng. Des.* **1982**, *67*, 245–258. [CrossRef]
39. Kodur, V.; Khaliq, W. Effect of Temperature on Thermal Properties of Different Types of High-Strength Concrete. *J. Mater. Civ. Eng.* **2011**, *23*, 793–801. [CrossRef]
40. Kodur, V.K.R. Performance-Based Fire Resistance Design of Concrete-Filled Steel Columns. *J. Constr. Steel Res.* **1999**, *51*, 21–36. [CrossRef]
41. Cheng, F.-P.; Kodur, V.K.R.; Wang, T.-C. Stress-Strain Curves for High Strength Concrete at Elevated Temperatures. *J. Mater. Civ. Eng.* **2004**, *16*, 84–90. [CrossRef]
42. Kodur, V.K.R.; Wang, T.C.; Cheng, F.P. Predicting the Fire Resistance Behaviour of High Strength Concrete Columns. *Cem. Concr. Compos.* **2004**, *26*, 141–153. [CrossRef]
43. Othuman Mydin, M.A.; Wang, Y.C. Thermal and Mechanical Properties of Lightweight Foamed Concrete at Elevated Temperatures. *Mag. Concr. Res.* **2012**, *64*, 213–224. [CrossRef]
44. Kodur, V.; McGrath, R. Fire Endurance of High Strength Concrete Columns. *Fire Technol.* **2003**, *39*, 73–87. [CrossRef]
45. Kanagaraj, B.; Kiran, T.; Jayakumar, G.; Anand, N.; Arulraj, P.; Gurupatham, B.G.A.; Roy, K. Performance of Sustainable Insulated Wall Panels with Geopol- Ymer Concrete. *Materials* **2022**, *15*, 8801. [CrossRef] [PubMed]
46. Wang, W.; Liu, X.; Guo, L.; Duan, P. Evaluation of Properties and Microstructure of Cement Paste Blended with Metakaolin Subjected to High Temperatures. *Materials* **2019**, *16*, 941. [CrossRef] [PubMed]
47. Nadeem, A.; Memon, S.A.; Lo, T.Y. Mechanical Performance, Durability, Qualitative and Quantitative Analysis of Microstructure of Fly Ash and Metakaolin Mortar at Elevated Temperatures. *Constr. Build. Mater.* **2013**, *38*, 338–347. [CrossRef]

48. Nadeem, A.; Memon, S.A.; Lo, T.Y. Qualitative and Quantitative Analysis and Identification of Flaws in the Microstructure of Fly Ash and Metakaolin Blended High Performance Concrete after Exposure to Elevated Temperatures. *Constr. Build. Mater.* **2013**, *38*, 731–741. [CrossRef]
49. Abdelmelek, N.; Alimrani, N.S.; Krelias, N.; Lubloy, E. Effect of Elevated Temperatures on Microstructure of High Strength Concrete Based-Metakaolin. *J. King Saud Univ.-Eng. Sci.* **2021**. [CrossRef]